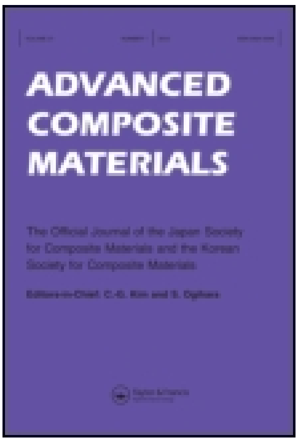

Advanced Composite Materials
Publication details, including instructions for authors and subscription information:
http://www.tandfonline.com/loi/tacm20

Full-field singular stresses in a composite laminate weakened by a cylindrical cavity: theory and experiment

Endel V. Iarve & David H. Mollenhauer

Version of record first published: 02 Apr 2012.

Adv. Composite Mater., Vol. 11, No. 1, pp. 21–29 (2002)

Full-field singular stresses in a composite laminate weakened by a cylindrical cavity: theory and experiment

ENDEL V. IARVE [1,*] and DAVID H. MOLLENHAUER[2]

[1] *University of Dayton Research Institute, 300 College Park Ave., Dayton, OH 45469, USA*
[2] *United States Air Force Research Laboratory, AFRL/MLBC, 2941 P Street Room 243, Wright Patterson AFB, Ohio 45433-7750, USA*

Abstract—Analytical and experimental investigation of strain fields arising in composite laminates in the vicinity of an open hole and ply interfaces was performed. The singular stress fields, arising at the ply interface and hole edge intersections, were analytically examined by using a novel technique based on superposition of an asymptotic and spline approximation solution. The moiré interferometry technique, providing high spatial resolution and allowing rapid strain variations across a laminate thickness to be recorded, was utilized to experimentally measure the strain distributions throughout the thickness of a $[+30_2/-30_2/90_4]_{3s}$ laminate. The singular solution and the experimentally measured strain showed good agreement for most strain components with some discrepancy for the interlaminar normal strain component.

Keywords: Composite material; hybrid analysis; variational method; moiré interferometry.

1. INTRODUCTION

Bolted joining remains a primary joining method of load carrying composite structural elements in modern aircraft. Significant efforts to develop methods for composite bolted joint strength prediction put forth in the past by government agencies [1], as well as proprietary programs [2], led to the development of several computer codes, which were adopted by various airframe and helicopter manufacturing companies as standard tools for composite bolted joint strength prediction. A common mechanical foundation for all of these tools is classical lamination theory combined with either stress or fracture mechanics failure criterion containing empirical geometric, material, and loading related constants needed to describe the experimentally obtained failure envelope. Definition of these empirical parameters requires extensive experimental effort.

*To whom correspondence should be addressed. E-mail: endel.iarve@wpafb.af.mil.

The objective of the present research is the development of analytical tools based on three-dimensional stress and failure analysis at the ply level. The present paper is focused on analytical and experimental characterization of the stress fields in laminated composites near singularities arising at the ply interface and hole intersections. The singular stress fields were analytically examined by using a novel technique based on superposition of an asymptotic and spline approximation solution, described in Iarve and Pagano [7]. The moiré interferometry technique, providing high spatial resolution and allowing rapid strain variations across a laminate thickness to be recorded, was utilized for experimental characterization.

A method of superposition of a hybrid and displacement approximation was developed to provide accurate stress fields in a multilayered composite laminate including the singular neighborhood of the ply interface and the hole edge. Asymptotic analysis was used to derive the hybrid stress functions. Morley [3] pioneered the idea of superposition of the analytical and finite element solutions in problems with local field singularities. Yamamoto and Tokuda [4] applied this method to crack stress intensity factor determination, using a multiple term asymptotic expansion for the analytical solution. They used a boundary collocation method to obtain the coefficients of the terms contained in the analytical solutions. Yamamoto and Sumi [5] considered an axisymmetric problem of a twisted round isotropic bar with an annular crack. The asymptotic solution, which was used as the basis for the analytical solution near the crack tip, was equivalent to a local plane strain solution, which does not satisfy the axisymmetric equilibrium equations throughout the domain. The asymptotic solution for the round isotropic bar problem, which was reduced to a single unknown function — the circumferential displacement component — was augmented by a higher-order term, added to the asymptotic solution to satisfy the equilibrium equations. However, in a general orthotropic case, these complementary terms are not obvious and have not been reported in the literature.

For the curvilinear edge singularities in orthotropic plies, considered in the present paper, the analytical solution in a finite domain near the singularity is unknown. The present paper extends the superposition approach to problems where no analytical solutions in the finite domain are known. The model developed is based on Reissner's variational principle and is intended to reflect the singularities that arise at each interface at the boundary of the hole. Hybrid approximation functions to be developed have the following characteristics:

(1) They include the asymptotic solution, thus representing the directional nonuniquiness of the solution. It is only in this manner that one can embed the proper singular field. The fact that the asymptotic solution results from the three-dimensional problem by truncating the spatial derivatives in the circumferential direction [6] will be used to construct hybrid stress functions.

(2) Two independent (B-spline) displacement functions are considered. One is related to the regular and the other to the singular portion of the stress field. It is undesirable to use the asymptotic displacement functions in the displacement approximation because the calculation of their derivatives in the circumferential

direction, required in the variational formulation, is only possible numerically. The displacements related to the singular stresses will be also approximated with splines. Thus the approximations of stresses and displacements are made independently.

2. PROBLEM DEFINITION

Consider a rectangular orthotropic laminate containing a circular hole having a diameter D. The laminate consists of N plies of total thickness H in the z-direction and has a length L in the x-direction and width A in the y-direction. An open hole of diameter D with the center at $x = x_c$ and $y = y_c$ is considered. Uniaxial stretching in the x-direction is applied via displacement $u_x = \mathrm{u}_0 > 0$ at $x = L$ and $u_x = 0$ at $x = 0$. A cylindrical coordinate system r, θ, z is introduced at the center of the hole, so that $\theta = 0$ is parallel to the x-axis.

2.1. Asymptotic analysis

A local coordinate system η, ψ, z, shown in Fig. 1, is introduced at the interface between plies s and $s + 1$. The origin is at the point $r = D/2$, $z = z^{(s)}$, θ so that η is the distance from a singular point, and ψ is an angle defining the direction in which the origin of the coordinates is approached: $-\pi/2 \leqslant \psi \leqslant 0$ belongs to the $s-$ply and $0 \leqslant \psi \leqslant \pi/2$-belongs to the $s + 1$-ply. Free-edge boundary conditions are imposed at $\psi = \pm\pi/2$, and displacement and traction continuity is imposed at $\psi = 0$. In the limit of $\eta \to 0$ the following asymptotes for the stress distribution were obtained, with the accuracy of an arbitrary multiplicative factor:

$$a_{ij}^m = \eta^{\lambda_m - 1} f_{ij}(\lambda_m, \psi, \theta). \tag{1}$$

The values of λ are determined to provide a nontrivial solution under the imposed boundary conditions.

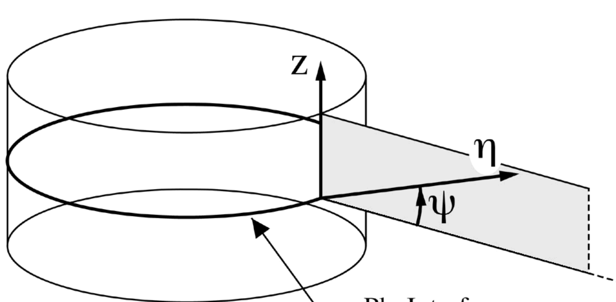

Figure 1. Coordinate system used in the asymptotic analysis.

2.2. Spline approximation of displacements

Cubic B-splines are used for the displacement approximation which, according to [6], can be written as:

$$u_i = \mathbf{C}_i \mathbf{X} \mathbf{U}_i^* + \delta_{ix} \mathbf{X} \mathbf{E}_0^* \cdot u_0, \tag{2}$$

where $\mathbf{X}$ is a vector of three-dimensional spline approximation basis functions. Superscript star denotes the transpose operation. Boundary matrices $\mathbf{C}_i$ and constant vector $\mathbf{E}_0$ are defined so that approximation (2) provides a kinematically admissible displacement field. Curvilinear coordinates ρ and ϕ, shown in Fig. 2, were introduced to map the laminate with a cutout into a region $0 \leqslant \rho \leqslant 1$ and $0 \leqslant \phi \leqslant 2\pi$. Vector $\mathbf{X}$ is a tensor product of one-dimensional basis spline functions of ρ, ϕ and z coordinates, respectively.

2.3. Hybrid approximation

It was shown by Iarve and Pagano [7] that it is beneficial to consider as independent displacement functions the total displacement (2) and the displacement u_{ij}^s related to the singular stresses. The singular displacement is approximated similar to (2), and the boundary condition matrices are defined to satisfy the condition of zero radial displacement at the hole edge. The hybrid stress approximation is proposed as follows

$$\sigma_{ij} = \sum_m K_m(\theta)\left(a_{ij}^m - s_{ij}^m\right) + \sigma_{ij}^u, \tag{3}$$

where σ_{ij}^u is calculated by using Hooke's law from displacements (2) and a_{ij}^m is given by equation (1). Functions s_{ij}^m are spline approximations of functions a_{ij}^m. They are defined by auxiliary solutions [7]. Unknown coefficients K_m are computed by requiring the stresses (3) to satisfy interlaminar σ_{rz} continuity at the collocation points.

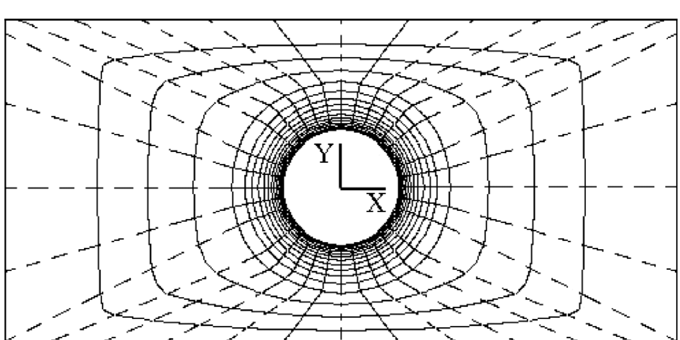

Figure 2. Curvilinear coordinate system; dashed lines represent ϕ = constant and solid lines represent $\rho = \text{constant}$.

3. MOIRÉ INTERFEROMETRY EXPERIMENTS

The free-edge strains in laminated composites were studied for curved surfaces. The research focused on the development and use of moiré interferometry techniques applied to the open hole problem in laminated composites. Moiré interferometry [8] was chosen because the excellent spatial resolution and full-field nature of this optical displacement measuring technique would allow rapid strain variations across a laminate thickness to be recorded. Three specimens were examined in this study. An aluminum specimen was used to develop and validate the experimental procedures. Two composite specimens, fabricated from IM7/5250-4 prepreg with ply lay-ups of $[0_4/90_4]_{3s}$ and $[30_2/-30_2/90_4]_{3s}$, were then examined with the refined techniques. The procedure required that a replica of the grating on the cylindrical surface of the hole be made while the specimen was loaded. This cylindrical-shaped deformed grating replica was then examined directly in a moiré interferometer. A schematic of this procedure is shown in Fig. 3. This multi-step procedure was developed mainly to eliminate an uncertainty associated with the θ-direction displacement variation. The resulting fringe patterns were narrow strips, approximately 3° wide, which were recorded at various angular locations around the hole. A mosaic of U_θ fringe patterns from $48^\circ - 69^\circ$ on the cylindrical surface of the $[30_2/-30_2/90_4]_{3s}$ specimen is shown in Fig. 4. Clearly, sub-ply variations of displacement can be obtained from these fringe patterns. Distributions of strain at various angular locations around the periphery of the holes were calculated from the recorded displacement fringe patterns. Representative results from the $[30_2/-30_2/90_4]_{3s}$ specimen are subsequently presented. A comprehensive report of the research can be found in [9], which is available for download from the World Wide Web; however, a less refined analytical solution was used for comparison in that work.

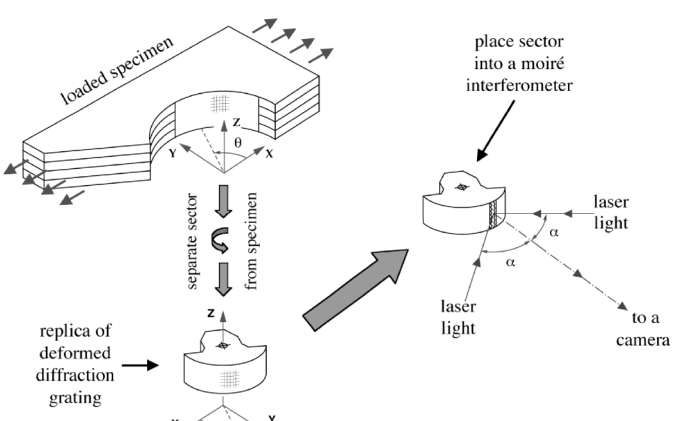

Figure 3. Schematic of the procedure for recording fringe patterns from the deformed curved specimen grating by examining a curved replica in a moiré interferometer.

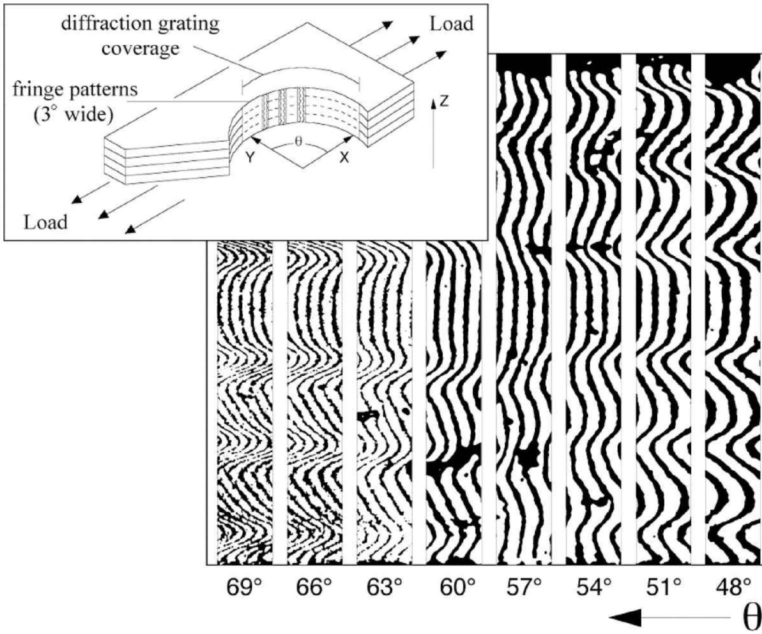

Figure 4. U_θ fringe pattern mosaic from the $[30_2/{-30_2}/90_4]_{3s}$ specimen.

4. RESULTS AND DISCUSSION

The convergence and accuracy of the numerical procedure are addressed in [6, 7]. Comparisons of the analytically and experimentally obtained interlaminar distributions of three strain components at the edge of an open hole in an IM7/5250-4 laminate are shown in Figs 5–7. The stacking sequence $[30_2/-30_2/90_4]_{3s}$ was utilized to enhance the interlaminar stress and strain values. The elastic properties of the unidirectional ply were $E_1 = 151$ GPa, $E_2 = E_3 = 9.45$ GPa, $G_{12} = G_{13} = 5.9$ GPa, $G_{23} = 3.26$ GPa, $\upsilon_{12} = \upsilon_{13} = 0.32$, and $\upsilon_{23} = 0.45$. The in-plane dimensions of the plate were $L = 0.147$ m, $A = 0.0736$ m, $x_c = L/2$, $y_c = A/2$, $D = 0.0254$ m and the ply thickness $h = 0.00134$ m. Uniaxial loading was applied in the x-direction with the far-field stress equal to 50 MPa.

The mesh was chosen so that $n_s = 1$ or one sublayer per ply in the z-direction; ρ-coordinate was subdivided into a total of $m = 16$ intervals, with $m_1 = 12$ intervals in the cylindrical transformation region, which was a hole radius wide ($\kappa\rho_h = 1$). The consecutive interval length ratio was $q = 1.2$, where $q = (\rho_{i+1} - \rho_i)/(\rho_i - \rho_{i-1})$. The θ coordinate in all cases was uniformly divided into 36 intervals.

Comparisons of the analytically and experimentally obtained distributions of three strain components at the edge of an open hole in laminate are presented in Figs 5–7. The analytical results on the figures are referred to as SVELT results, where SVELT is the software package implementing the theory described above. Distributions of ε at 66°, the $\gamma_{\theta z}$ component at 75°, and the ε_z at 90° are compared with predictions

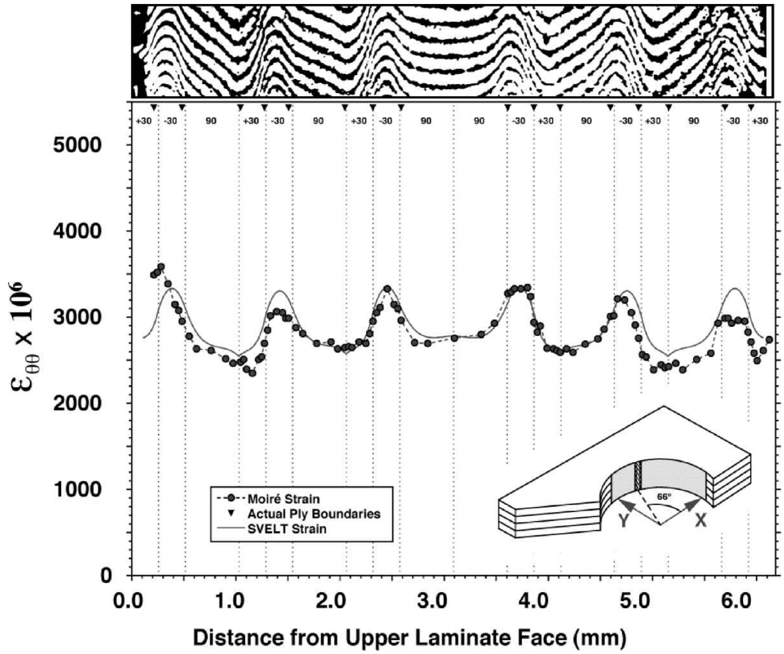

Figure 5. Comparison of the distribution of ε_θ through the laminate thickness at 66° for the $[30_2/-30_2/90_4]_{3s}$ laminate.

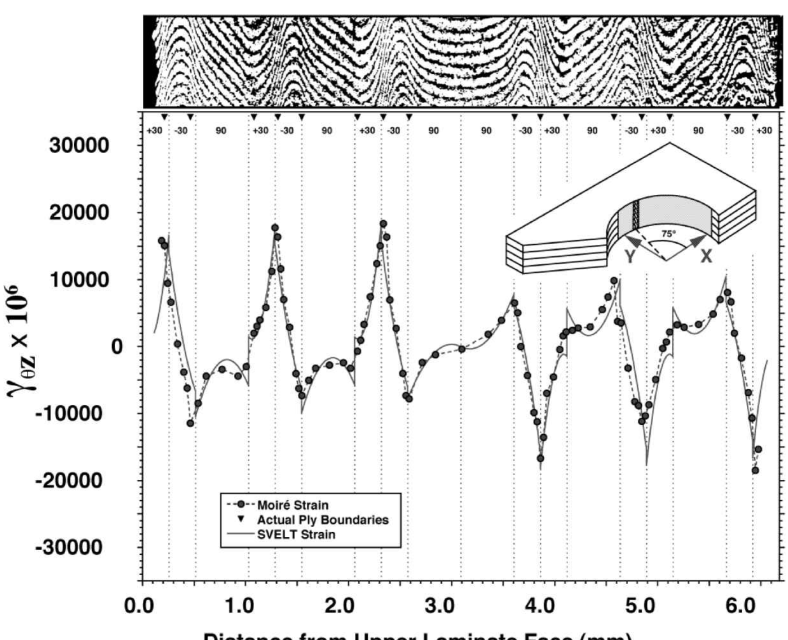

Figure 6. Comparison of the distribution of $\gamma_{\theta z}$ through the laminate thickness at 75° for the $[30_2/-30_2/90_4]_{3s}$ laminate.

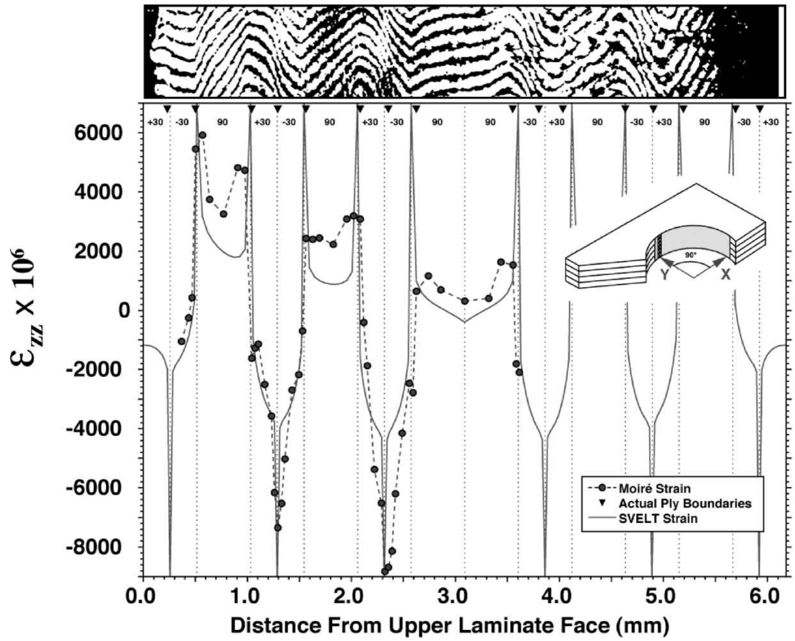

Figure 7. Comparison of the distribution of ε_z through the laminate thickness at 90° for the $[30_2/-30_2/90_4]_{3s}$ laminate.

made with the present model. Within these figures, the vertical dotted lines represent the idealized ply boundaries. The filled triangles represent the approximate ply boundaries of the actual specimen. The numbers across the top of these charts represent the fiber orientation of the particular ply. The results from the experiment and the numerical model are extremely close for ε_θ and $\gamma_{\theta z}$. It is worthwhile to point out the difference of the two strain component distribution patterns, i.e. ε_θ has a smooth thickness distribution, whereas the $\gamma_{\theta z}$ component has sharp peaks at the ply interfaces. It is in agreement with the theoretical prediction that the hoop strain component is bounded and $\gamma_{\theta z}$ exhibits singular behavior. Similar verification is found at all angular locations examined. The present model accurately predicts the strain trends and strain magnitudes measured by moiré. The comparison between the model predictions and moiré for ε_z is not as close. The strain trends measured by the moiré experiments are closely matched by the spline model prediction; however, the strains are consistently lower in magnitude than the moiré measurements. This discrepancy is under investigation. The suspected cause is the discrepancy between the transverse normal stiffness of the specimen and the value used in the model, although a micromechanical origin is also being considered.

5. CONCLUSIONS

Singular full-field stress distribution in composite laminates with open holes was obtained by using a novel technique based on superposition of hybrid and displacement approximation. Moiré interferometric measurements of the through-the-thickness distribution of strain components inside the hole of a $[30_2/-30_2/90_4]_{3s}$ laminate were performed. Very close agreement of the theoretical and experimental results was observed for the hoop and interlaminar transverse shear strain components. Some quantitative difference for the interlaminar normal strain component is under investigation.

REFERENCES

1. D. S. Snyder, J. G. Burns and V. B. Venkayya, Composite bolted joints analysis programs, *J. Compos. Technol. Res.* **12**, 41–51 (1990).
2. J. R. Eisenmann, Bolted joint static strength model for composites materials, in: *Third Conference on Fibrous Composite Materials in Flight Vehicle Design, Part II* (NASA TM X-3377) (1976).
3. L. S. D. Morley, A finite element application of the modified Rayleigh-Ritz method, *Int. J. Numer. Methods Engng* **2**, 85–98 (1970).
4. Y. Yamamoto and N. Tokuda, Determination of stress intensity factors in cracked plates by the finite element method, *Int. J. Numer. Methods Engng* **6**, 427–439 (1973).
5. Y. Yamamoto and Y. Sumi, Stress intensity factors for three-dimensional cracks, *Int. J. Fracture* **14**, 17–38 (1978).
6. E. V. Iarve, Spline variational three dimensional stress analysis of laminated composite plates with open holes, *Int. J. Solids Structures* **33**, 2095–2117 (1996).
7. E. V. Iarve and N. J. Pagano, Singular full-field stresses in composite laminates with open holes, *Int. J. Solids Structures* (2000) (in press).
8. D. Post, B. Han and P. Ifju, *High Sensitivity Moiré: Experimental Analysis for Mechanics and Materials.* Springer-Verlag, New York (1994).
9. D. H. Mollenhauer, Interlaminar deformation at a hole in laminated composites: a detailed experimental investigation using moiré interferometry, Doctor of Philosophy Dissertation available for download at the Virginia Polytechnic Institute and State University library's Web page http://scholar.lib.vt.edu/theses/theses.html (1997).